JOURNAL OF COMPUTATIONAL PHYSICS 49, 334–341 (1983)

Note

Numerical Calculations of Discontinuities by Shape Preserving Splines

Methods to interpolate one dimensional data by constructing a visually pleasing monotone interpolant free from the "bumps" and "wiggles" that frequently plague standard interpolation methods have been the subject of several publications in recent years (see the work of Fritsch and Carlson, where the problem of monotone piecewise cubic interpolation has been studied and compared to other standard interpolation methods [1]). A related problem is that of integrating differential equations in an Eulerian mesh when the solution of the equation

$$(\partial u/\partial t) + c(\partial u/\partial x) = 0 \tag{1}$$

is calculated from the equation

$$u(x, t) = u(x - ct, 0) \tag{2}$$

by polynomial interpolation. The "bumps" and "wiggles" which result in this case is the presence of discontinuities and shocks create troubles. Hyperbolic equations of the type in Eq. (1) are of fundamental importance in many branches of mathematical physics. (The solution of the Vlasov equation by splitting techniques can be reduced to the problem of solving equations of the type in Eq. (1) [2–3].) The problem of solving Eq. (1) by polynomial interpolation has been studied recently by Knorr and Mond [4], who applied a monotonicity principle in addition to a cubic spline interpolation. This monotonicity principle makes use of the fact that if the solution $u(x, t)$ or a part of it is monotone at time t, it will remain so for later times, and hence this principle is enforced to eliminate any deformation, and to keep or restore the monotone shape of the curve. (A review of alternative methods for the solution of Eq. (1), such as FCT [5], is also presented in [4].) When, however, such a monotonicity principle is applied to the solution of equations like the Vlasov equation, where very small localized bumps and irregularities can develop due to nonlinear effects such as wave-particle interactions, and with small structures developing in the phase-space fluid, special care and attention is to be paid when such a monotonicity principle is applied.

Shape preserving polynomial or spline interpolation has been investigated by several authors in recent years [6–7], and can offer a nice alternative for the solution of problems of the type discussed, without any additional external modification, deformation, or correction introduced to the algorithm. An algorithm for the

0021-9991/83/020334–08$03.00/0

computation of an interpolating shape-preserving osculatory quadratic spline has been presented in [7]. This quadratic spline preserves the monotonicity and convexity of the data when consistent with the given derivatives at the data points. It is the purpose of this note to apply such an algorithm for the solution of the problems discussed.

Details for the algorithm can be found in [7]. We give for reference the essential steps to compute the quadratic spline in order to fix the notation. The method depends on the following property of the Bernstein polynomials on an interval $I = [x_i, x_{i+1}]$: Let $P(x_i, y_i)$ and $Q(x_{i+1}, y_{i+1})$ denote the end points of interval I. Let $T(x_T, y_T)$ be a point satisfying $x_T = (x_i + x_{i+1})/2$. Let g be the first degree spline passing through the points $P(x_i, y_i)$, $Q(x_{i+1}, y_{i+1})$, and T, with a single knot at x_T. Let $B_2(g)(x)$ be the second degree Bernstein polynomial of g on $[x_i, x_{i+1}]$, which we denote by

$$B_2(P, T, Q) = (x_{i+1} - x_i)^{-2}\{g(x_i)(x_{i+1} - x)^2 + 2y_T(x - x_i)(x_{i+1} - x) + g(x_{i+1})(x - x_i)^2\}. \tag{3}$$

Then:

(1)

$$B_2(g)(x_i) = g(x_i) = y_i, \tag{4}$$

$$B_2(g)(x_{i+1}) = g(x_{i+1}) = y_{i+1}, \tag{5}$$

(2)

$$B_2'(g)(x_i) = g'(x_i), \tag{6}$$

$$B_2'(g)(x_{i+1}) = g'(x_{i+1}). \tag{7}$$

(3) If g is monotone on $[x_i, x_{i+1}]$, then $B_2(g)$ is monotone on the same interval.

(4) If g is convex (concave) on $[x_i, x_{i+1}]$, then $B_2(g)$ is convex (concave) on the same interval.

Hence $B_2(g)$ preserves the shape of g, has a continuous first derivative on $[x_i, x_{i+1}]$, while g does not.

We use this property to construct a first-degree spline g on I, which has slope M_i at P and M_{i+1} at Q. Let L_1 be the line through P with slope M_i and L_2 the line through Q of slope M_{i+1}. (See Fig. 1.) Let x_z be the abscissa of the point of intersection of L_1 and L_2. Let $V(x_V, y_V)$ and $W(x_W, y_W)$ be the points of abscissa

$$x_V = (x_i + x_z)/2, \tag{8}$$

$$x_W = (x_z + x_{i+1})/2 \tag{9}$$

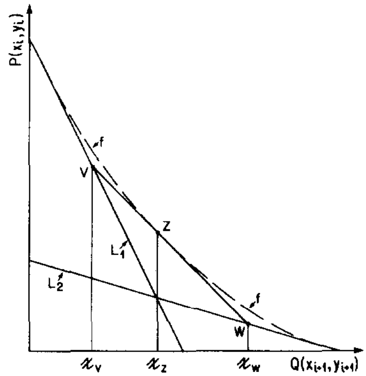

FIG. 1. The interval $P(x_i, y_i)$, $Q(x_{i+1}, y_{i+1})$ which is interpolated by Eq. (13).

situated, respectively, on lines L_1 and L_2

$$y_V = L_1(x_i + x_z)/2, \tag{10}$$

$$y_W = L_2(x_z + x_{i+1})/2. \tag{11}$$

Let L be the line joining V and W and define

$$y_z = L(x_z). \tag{12}$$

Then $Z(y_z, x_z)$ is a join point on the spline. Define f on $[x_i, x_{i+1}]$ as follows:

$$\begin{aligned} f(x) &= B_2(P, V, Z), \qquad \text{on} \quad [x_i, x_z], \\ &= B_2(Z, W, Q), \qquad \text{on} \quad [x_z, x_{i+1}]. \end{aligned} \tag{13}$$

Then $f \in C^1[x_i, x_{i+1}]$ and satisfies

$$f(x_i) = y_i, \tag{14}$$

$$f(x_{i+1}) = y_{i+1}, \tag{15}$$

$$f'(x_i) = M_i, \tag{16}$$

$$f'(x_{i+1}) = M_{i+1}. \tag{17}$$

If L_1 and L_2 intersect at x_z outside $[x_i, x_{i+1}]$, then we take $x_z = (x_i + x_{i+1})/2$. For other particular cases, see [7]. The method used in [7] to determine M_i, and which we apply in the following calculations is the following: Let S_i be the quantity

$$S_i = (y_i - y_{i-1})/(x_i - x_{i-1}) \qquad \text{for} \quad i = 1, 2, \ldots, N. \tag{18}$$

If $|S_i| > |S_{i+1}| > 0$, we extend the line through (x_i, y_i) of slope S_i until it intersects the horizontal line through (x_{i+1}, y_{i+1}) at the point $(\bar{x}, y_{i+1})$. We set $\hat{x} = (\bar{x} + x_{i+1})/2$

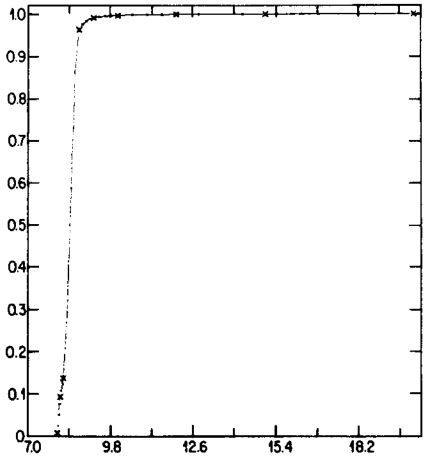

FIG. 2. The interpolation curve for the first data set from [1]. The crosses denote the data points.

and $M_i = (y_{i+1} - y_i)/(\hat{x} - x_i)$. On the other hand, if $0 < |S_i| < |S_{i+1}|$, we reverse the procedure by extending the line through (x_i, y_i) of slope S_{i+1}, until it intersects the horizontal line through (x_{i-1}, y_{i-1}) at the point $(\bar{x}, y_{i-1})$. Then we set $\hat{x} = (x_{i-1} + \bar{x})/2$ and $M_i = (y_i - y_{i-1})/(x_i - \hat{x})$. For other particular cases, see [7].

Figures 2–4 contain the interpolation curves for three data sets. The first two data sets (Figs. 2 and 3) labeled RPN 12 and RPN 14 in [1], are actual data from LLL radiochemical calculations, while the data set in Fig. 4 is taken from Akima [8]. (The crossed points are the data sets, the other points are interpolated points using Eq. (13).) The resultant curves appear smooth and natural.

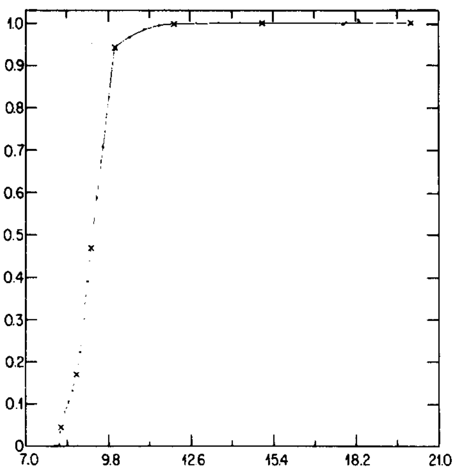

FIG. 3. The interpolation curve for the second data set from Ref. [1]. The crosses denote the data points.

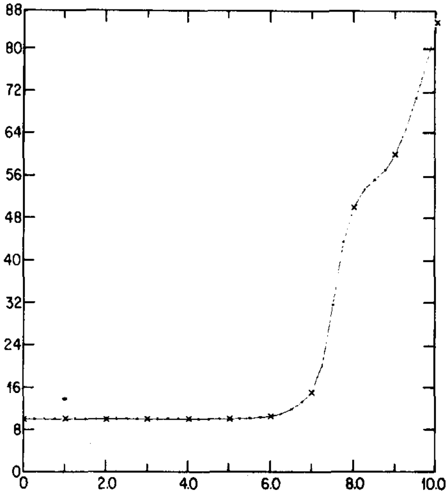

FIG. 4. The interpolation curve for the data set from Ref. [8]. The crosses denote the data point.

We use Eq. (13) to propagate a unit pulse according to Eq. (1) with $\varepsilon = c\Delta t/\Delta x = 0.2$, where Δt is the time step and Δx is the uniform mesh size. The result is shown in Figs. 5a and b for the case with 50 points (after 500 time steps and 1000 time steps, respectively). The flanks of the discontinuities remained smooth. Figure 6 contains the same test in which $\varepsilon = 0.1$. To reach the same time as in Figs. 5, we have to run the code for 2000 time steps. Since the method is very sensitive to the calculation of the derivatives as indicated in Eq. (18), we have used as a value for the derivative the geometric mean between the value obtained when using Eq. (18) and the value calculated from a cubic spline (very little difference is

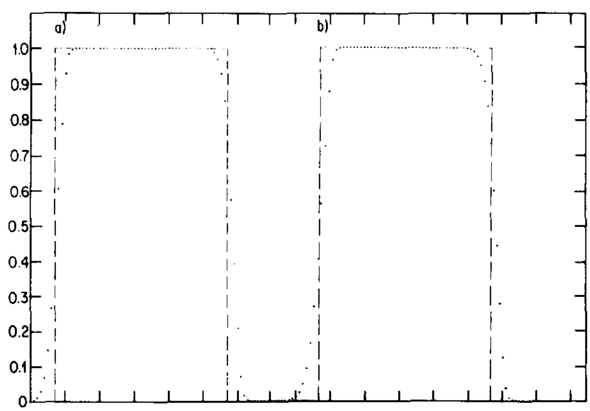

FIG. 5. The propagation of a pulse following Eq. (1), with $N = 50$ points (a) after 500 time steps, (b) after 1000 time steps. Note: $c\Delta t/\Delta x = 0.2$.

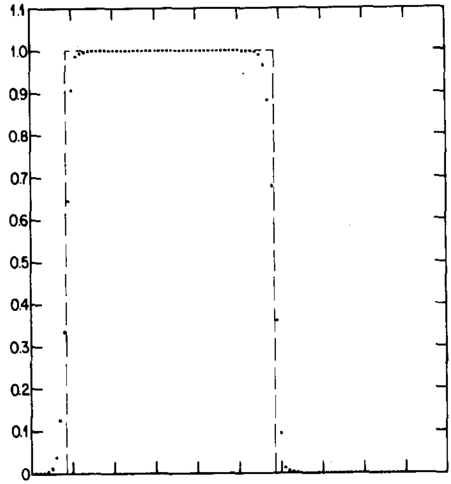

FIG. 6. The propagation of a pulse following Eq. (1), with $N = 50$ points, after 2000 time steps. Note: $c\Delta t/\Delta x = 0.1$.

observed if only the value obtained by the method following Eq. (18) is used for the derivatives). Absolutely no bumps or overshooting appear. The erosion of the edges has been reduced. The form of the pulse remained highly symmetric: if we except the small rounding of the corners, only five points are appearing on the vertical line. The area of the unit pulse, calculated by a simple summation rule, varied between 0.999 and 1.000, indicating that the deformation of the corners is very symmetric. So, at the expense of a small additional computational effort, very accurate results are obtained by a single quadratic polynomial interpolation.

Figure 7 contains the results obtained with a sine test, a sine wave interrupted by a

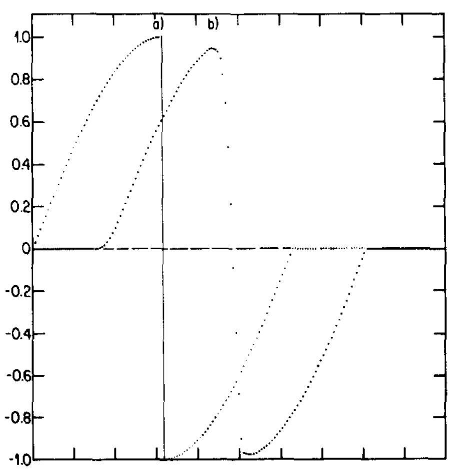

FIG. 7. The propagation of a discontinuous sine curve following Eq. (1), (a) at $t = 0$; (b) after 500 time steps. Note: $c\Delta t/\Delta x = 0.2$.

discontinuity, as in [4]. The discontinuity remained located where it should be, according to the solution in Eq. (2), and the shape of the sine remained very nicely conserved. The discontinuity has broadened slightly and the amplitude of the positive peak has decreased by about 7% and by about 2.5% for the negative peak after 500 time steps.

The accuracy of the method is further demonstrated by integrating the hydrodynamic equations written in terms of the Riemann invariants α and β [9], for the case of an isentropic flow,

$$(\partial\alpha/\partial t) + (u + c)\,\partial\alpha/\partial x = 0, \tag{19}$$

$$(\partial\beta/\partial t) + (u - c)\,\partial\beta/\partial x = 0, \tag{20}$$

where

$$u = \tfrac{1}{2}(\alpha - \beta), \tag{1}$$

$$c = \tfrac{1}{4}(\gamma - 1)(\alpha + \beta). \tag{22}$$

Equations (19) and (20) are of form (1) and are integrated using the previous method on a predictor–corrector scheme. We chose $\gamma = 1.4$. Our initial conditions assume $u = 0$ everywhere, with two constant states, one to the left and one to the right, separated by a discontinuity which is assumed to lie midway two grid points. We use a uniform mesh with $\Delta x = 0.01$ and $\Delta t = 5 \times 10^{-3}$. The results in Figs. 8a and b for c and u, respectively, are obtained after 50 time steps. The schock region is very steep and is represented by two to three zones. Absolutely no overshooting is observed at the corners, which show very little erosion.

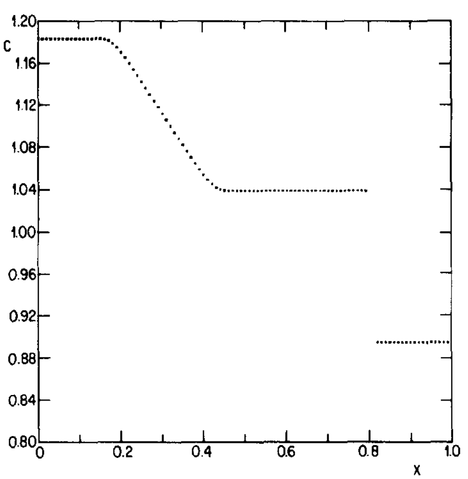

FIG. 8a. The plot of c for the solution of an isentropic flow as described in Eqs. (19) and (20) after 50 time steps.

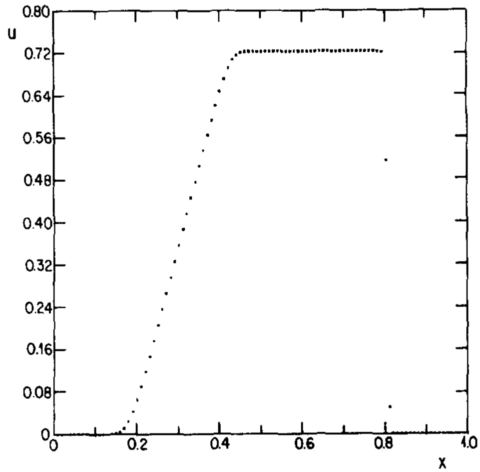

FIG. 8b. The plot of u for the solution of an isentropic flow as described in Eqs. (19) and (20) after 50 time steps.

An important point in the accuracy of the method is the choice of the additional knot x_z. Several particular cases are discussed in [7], especially when two additional knots are needed.

We conclude that problems of polynomials interpolations, especially when applied to the solution of differential equations similar to Eq. (1) with discontinuities and shocks, can be handled very nicely by shape preserving polynomial splines.

REFERENCES

1. F. N. FRITSH AND R. E. CARLSON, "Monotone Piecewise Cubic Interpolation," Lawrence Livermore Laboratory, Report UCRL-82453, 1979.
2. C-Z. CHENG AND G. KNORR, *J. Comput. Phys.* **22** (1976), 330.
3. M. M. SHOUCRI AND R. R. J. GAGNÉ, *J. Comput. Phys.* **27** (1978), 315.
4. G. KNORR AND M. MOND, *J. Comput. Phys.* **38** (1980), 212.
5. J. P. BORIS AND D. L. BOOK, *in* "Methods in Computational Physics," p. 85, Academic Press, New York, 1978; also S. T. ZALESAK, "High Order *Zip* Differencing of Convective Terms," Naval Research Laboratory, Memorandum Report 4218, 1980.
6. D. F. MCALLISTER, E. PASSOW, AND J. A. ROULIER, *Math. Comp.* **31** (1977), 717.
7. D. F. MCALLISTER AND J. A. ROULIER, *ACM Trans. Math. Software* **7** (1981), 331.
8. H. AKIMA, *J. Assoc. Comput. Mach.* **17** (1970), 589.
9. R. COURANT AND K. O. FRIEDRICHS, "Supersonic Flow and Shock Waves," Interscience, New York 1948.

RECEIVED: March 16, 1982; REVISED: July 15, 1982

MAGDI M. SHOUCRI

Institut de Recherche de L'Hydro-Quebec,
Varennes, JOL 2PO Quebec, Canada